Available online at www.sciencedirect.com
ScienceDirect
Information Fusion 9 (2008) 176–185
INFORMATION FUSION
www.elsevier.com/locate/inffus

Medical image fusion using *m*-PCNN

Zhaobin Wang, Yide Ma *

School of Information Science and Engineering, Lanzhou University, Lanzhou City, 730000 Gansu Province, China

Received 21 December 2006; received in revised form 4 April 2007; accepted 4 April 2007
Available online 19 April 2007

Abstract

Medical image fusion plays an important role in clinical applications such as image-guided surgery, image-guided radiotherapy, non-invasive diagnosis, and treatment planning. Pulse coupled neural network (PCNN) is derived from the synchronous neuronal burst phenomena in the cat visual cortex. However, it is very difficult to directly apply original PCNN into the field of image fusion, because its model has some shortcomings. Although a significant amount of research work has been done in developing various medical image algorithms, one disadvantage with the approaches is that they cannot deal with different kinds of medical images. In this instance, we propose a novel multi-channel model – *m*-PCNN for the first time and apply it to medical image fusion. In the paper, firstly the mathematical model of *m*-PCNN is described, and then dual-channel model as a special case of *m*-PCNN is introduced in detail. In order to show that the *m*-PCNN can deal with multimodal medical images, we used four pairs of medical images with different modalities as our experimental subjects. At the same time, in comparison with other methods (Contrast pyramid, FSD pyramid, Gradient pyramid, Laplacian pyramid, etc.), the performance and relative importance of various methods is investigated using the Mutual Information criteria. Experimental results show our method outperforms other methods, in both visual effect and objective evaluation criteria.

Keywords: PCNN; Medical image fusion; Image processing; Quality assessment; Multimodal image

1. Introduction

Recently, the study of multimodal medical image fusion has attracted more attention due to the increasing demands of clinical applications. Medical image fusion helps physicians extract the features that may not be normally visible in images by different modalities (e.g., MRI-T1 gives greater detail of anatomical structures, whereas MRI-T2 gives greater contrast between normal and abnormal tissues). Thus, in order to extract more information, medical image fusion combines these contrasting and complimentary features into one fused image. Medical image fusion not only helps in diagnosing diseases, but it also reduces the storage cost by reducing storage to a single fused image instead of multiple-source images.

People have proposed many approaches, such as FSD pyramid [1], gradient pyramid [2], Laplacian pyramid [3], DWT pyramid [4], SIDWT pyramid [5], morphological pyramid [6], ratio pyramid [7], contrast pyramid [8], and so on. All the above methods share one characteristic: each method is efficient for specific types of images and each approach has its own limits. For example, contrast pyramid method loses too much information from the source images in the process of fusion; ratio pyramid method produces lots of false information that does not exist in the source images; and morphological pyramid method creates many bad edges. In a word, these methods cannot deal with various types of medical images. In this paper, we propose a new method of medical image fusion using pulse coupled neural network (PCNN), which overcomes these limits.

PCNN is a biologically inspired neural network based on the work by Eckhorn et al. [9,10]. Pioneering work in the implementation of these algorithms was done by Johnson and his colleagues [11–16]. It has been proven that PCNN is very suitable for image processing [15,16] such as image segmentation, image enhancement, pattern

* Corresponding author. Tel.: +86 931 8912786; fax: +86 931 8912779.
E-mail address: ydma@lzu.edu.cn (Y. Ma).

1566-2535/$ - see front matter © 2007 Elsevier B.V. All rights reserved.
doi:10.1016/j.inffus.2007.04.003

recognition, etc. Researchers have developed some image fusion algorithms based on PCNN [17,18]; however, all the image fusion methods using PCNN have one common trait: one PCNN cannot finish the whole process of image fusion. Usually, a group of more than two PCNNs must be used to fuse multi-source images, making it inefficient and impractical, especially for a real-time system.

Analysis of the PCNN exposes a defect preventing one PCNN from fusing multi-source images. To make up for this defect, a new improved model, called *m*-PCNN, is proposed for the first time in this paper. Note: *m* indicates the number of external input channels. This model overcomes some limits of the original model in the data fusion. A remarkable characteristic of *m*-PCNN is that the number of external channels can easily be changed according to actual requirements, and is very useful when several images are fused at the same time. Therefore, *m*-PCNN successfully solves the problem of fusing multimodal images using only one PCNN. It has been proven here by experimental results that *m*-PCNN does well in the fusion of multimodal medical images.

The rest of this paper is organized as follows. In the next section, the original PCNN is briefly reviewed, and then the *m*-PCNN and its particular case are introduced, respectively. Section 3 describes an image fusion algorithm based on *m*-PCNN. Section 4 gives experimental results and evaluates the performance of various methods. Conclusions and future work are summarized at the end.

2. The model of *m*-PCNN

In this section, a brief review of the original PCNN is given, and then the *m*-PCNN model is introduced, which is proposed here for the first time. As a special case, the dual-channel PCNN is subsequently described.

2.1. PCNN model

In the original PCNN model, the PCNN neuron consists of three parts: dendritic tree, linking modulation, and pulse generator, as shown in Fig. 1.

The role of the dendritic tree is to receive the inputs from two kinds of receptive fields. Depending on the type of the receptive field, it is subdivided into two channels (the linking and the feeding). The linking receives external stimulus, while the feeding receives external stimulus and local stimulus.

In the following expressions, the indexes i and j refer to the pixel location in the image, k and l refer to the dislocation in a symmetric neighborhood around a pixel, and n denotes the current iteration (discrete time step). Here n varies from 1 to N (N is the total number of iterations).

The dendritic tree is given by:

$$F_{i,j}[n] = \exp(-\alpha_F)F_{i,j}[n-1] + V_F \sum_{k,l} m_{ijkl} Y_{i,j}[n-1] + S_{i,j} \tag{1}$$

$$L_{i,j}[n] = \exp(-\alpha_L)L_{i,j}[n-1] + V_L \sum_{k,l} w_{ijkl} Y_{i,j}[n-1] \tag{2}$$

The two main components F and L are called feeding and linking, respectively. M and W are the constant synaptic weights and S is the external stimulus. V_F and V_L are normalizing constants. α_F and α_L are the time constants; generally, $\alpha_F < \alpha_L$.

In the linking modulation, output is gathered from two channels. It is made by adding a bias to the linking and multiplying this by the feeding. The linking modulation is given by:

$$U_{i,j}[n] = F_{i,j}[n](1 + \beta L_{i,j}[n]) \tag{3}$$

In Eq. (3), $U_{i,j}[n]$ is the internal state of the neuron. β is the linking parameter and the pulse generator determines the firing events in the model in Eq. (4). $Y_{i,j}[n]$ depends on the internal state and threshold.

$$Y_{i,j}[n] = \begin{cases} 1, & U_{i,j}[n] > T_{i,j}[n] \\ 0, & \text{otherwise} \end{cases} \tag{4}$$

The dynamic threshold of the neuron is defined as

$$T_{i,j}[n] = \exp(-\alpha_T)T_{i,j}[n-1] + V_T Y_{i,j}[n] \tag{5}$$

Here V_T and α_T are normalized constant and time constant, respectively.

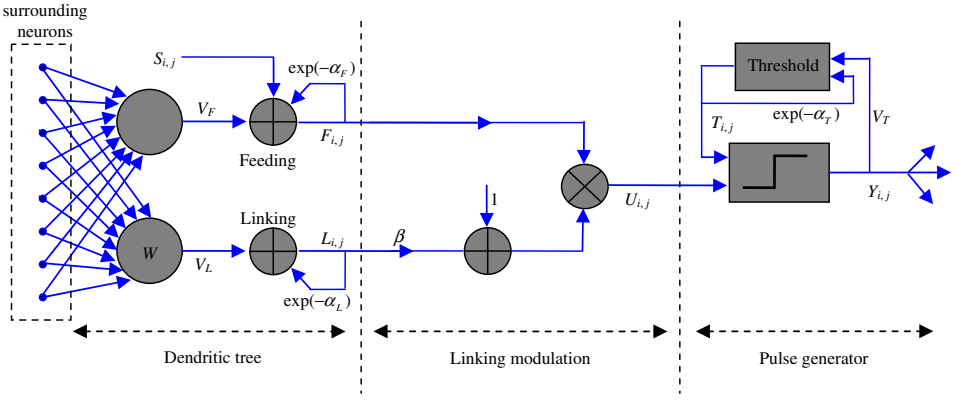

Fig. 1. The neuromime of PCNN.

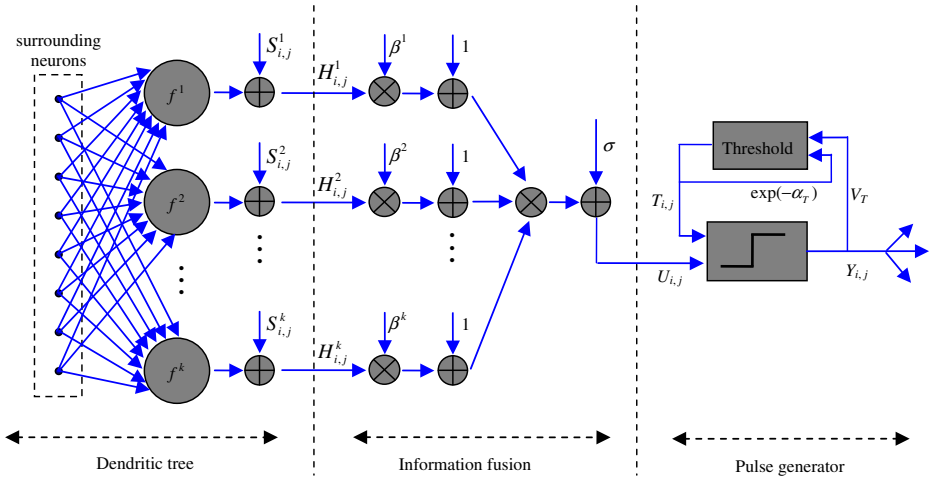

Fig. 2. The neuromime of *m*-PCNN.

This is a brief review of original PCNN. More details about PCNN will be found in the literatures [15,16].

2.2. m-PCNN

Undoubtedly, only one stimulus for each neuron is an obstacle for multiple-image fusion using the original PCNN. In order to correct this defect we, based on the original PCNN, propose a new improved model, called *m*-PCNN, as shown in Fig. 2. Like the original PCNN neuron, each *m*-PCNN neuron also consists of three parts: dendritic tree, information fusion, and pulse generator. The role of the dendritic tree is to receive two kinds of inputs. One is from the external stimulus and another is from the surrounding neurons. Information fusion is the place where all data is fused. The role of the pulse generator is to generate output pulse.

Compared with the original model, our model can adjust the number of external input channels according to practical demands. In the *m*-PCNN there are m input channels; generally, $m > 1$. So both stimuli can be input into the model at the same time. The following expressions mathematically describe its model.

$$H^k_{i,j}[n] = f^k(Y[n-1]) + S^k_{i,j} \tag{6}$$

$$U_{i,j}[n] = \prod_{k=2}^{K}(1 + \beta^k H^k_{i,j}[n]) + \sigma \tag{7}$$

$$Y_{i,j}[n] = \begin{cases} 1, & U_{i,j}[n] > T_{i,j}[n-1] \\ 0, & \text{otherwise} \end{cases} \tag{8}$$

$$T_{i,j}[n] = \exp(-\alpha_T)T_{i,j}[n-1] + V_T Y_{i,j}[n] \tag{9}$$

In these equations, H^k refers to the channel of the kth external input, S^k, $k = 2, 3, \ldots, K$ (presume K is the total number of external inputs) and $f^k(\cdot)$ is the feed function, which shows the influence of surrounding neurons on the current neuron. β^k refers to the weighting factor of the kth channel; usually, $0 < \beta^k < 1$. The value of β^k indicates the importance of the kth channel. If one source image plays a more important role in a system than the others, its corresponding value of β^k can be increased to stress its importance. If all the inputs have parallel importance, the factors usually will be set to the same constant. σ is the level factor to adjust the average level of internal activity. Other parameters are the same as parameters in the above PCNN.

In the process of image fusion, *m*-PCNN is a single layer two-dimensional array of laterally linked neurons and all neurons are identical. The number of neurons in the network is equal to the number of pixels in each input image. There exists a one-to-one correspondence between the pixels in each image and neurons. The gray value of a pixel is taken as the stimulus of the neuron. For a neuron, its stimuli come from the corresponding pixels in different images, which have the same position. Data fusion happens in the internal state of the neuron. Note: external input images must be registered and all inputs should also have identical resolution. Otherwise, image fusion makes no sense.

2.3. Dual-channel model

When there are only two external inputs, dual-channel PCNN is used. In fact, this case is often discussed in the literature, so it is necessary to explain it. The dual-channel

Table 1
Entropy of all original images

Images	Fig. 3(1)	Fig. 3(2)	Fig. 5(1)	Fig. 5(2)	Fig. 7(1)	Fig. 7(2)	Fig. 9(1)	Fig. 9(2)
	1.7126	5.6561	5.6278	5.7906	4.3699	4.5280	2.8458	4.6773

PCNN is a special case of m-PCNN, where $m = 2$. Now we will specifically explain the model, which is described strictly in the following expressions:

$$H^1_{i,j}[n] = M(Y[n-1]) + S^1_{i,j} \tag{10}$$

$$H^2_{i,j}[n] = W(Y[n-1]) + S^2_{i,j} \tag{11}$$

$$U_{i,j}[n] = (1 + \beta^1 H^1_{i,j}[n])(1 + \beta^2 H^2_{i,j}[n]) + \sigma \tag{12}$$

$$Y_{i,j}[n] = \begin{cases} 1, & U_{i,j}[n] > T_{i,j}[n-1] \\ 0, & \text{else} \end{cases} \tag{13}$$

$$T_{i,j}[n] = \exp(-\alpha_T) T_{i,j}[n-1] + V_T Y_{i,j}[n] \tag{14}$$

The dual-channel PCNN, as the name implies, has two external input channels. Let H^1 and H^2 stand for two symmetrical channels of current neurons. Their formulas are shown in Eqs. (10) and (11), where $M(\cdot)$ and $W(\cdot)$ are feed functions. Those functions indicate the influence of surrounding neurons on current neurons. Eq. (13) explains the internal state of the neuron, where β^1 and β^2 are the weighting coefficients of H^1 and H^2, respectively.

Using m-PCNN, multiple-source images are processed by single PCNN. Multiple external stimuli work in a neuron at the same time, which makes multiple-images processed in a parallel way. This saves time in the process of image fusion and cuts down computational complexity, as well.

3. Image fusion algorithm

PCNN has been applied to the domain of image fusion for several years; however, all of the proposed methods are characteristically complicated and inconvenient and cannot be applied in practice. However, m-PCNN solves this problem and makes the process of image fusion very simple, convenient, and efficient. Our method is shown as follows:

(1) Multi-source images are taken as multiple stimuli of m-PCNN. Let I^k denote multi-source images, generally $k > 1$. Namely $S^k = I^k$. Note: all external input images must be registered and also have the same size and identical resolution.
(2) Stimuli and feed information are transmitted into the neuron via their different channels.
(3) All received signals are mixed together in the internal activity of the neuron. From Eq. (7) or (12), there are

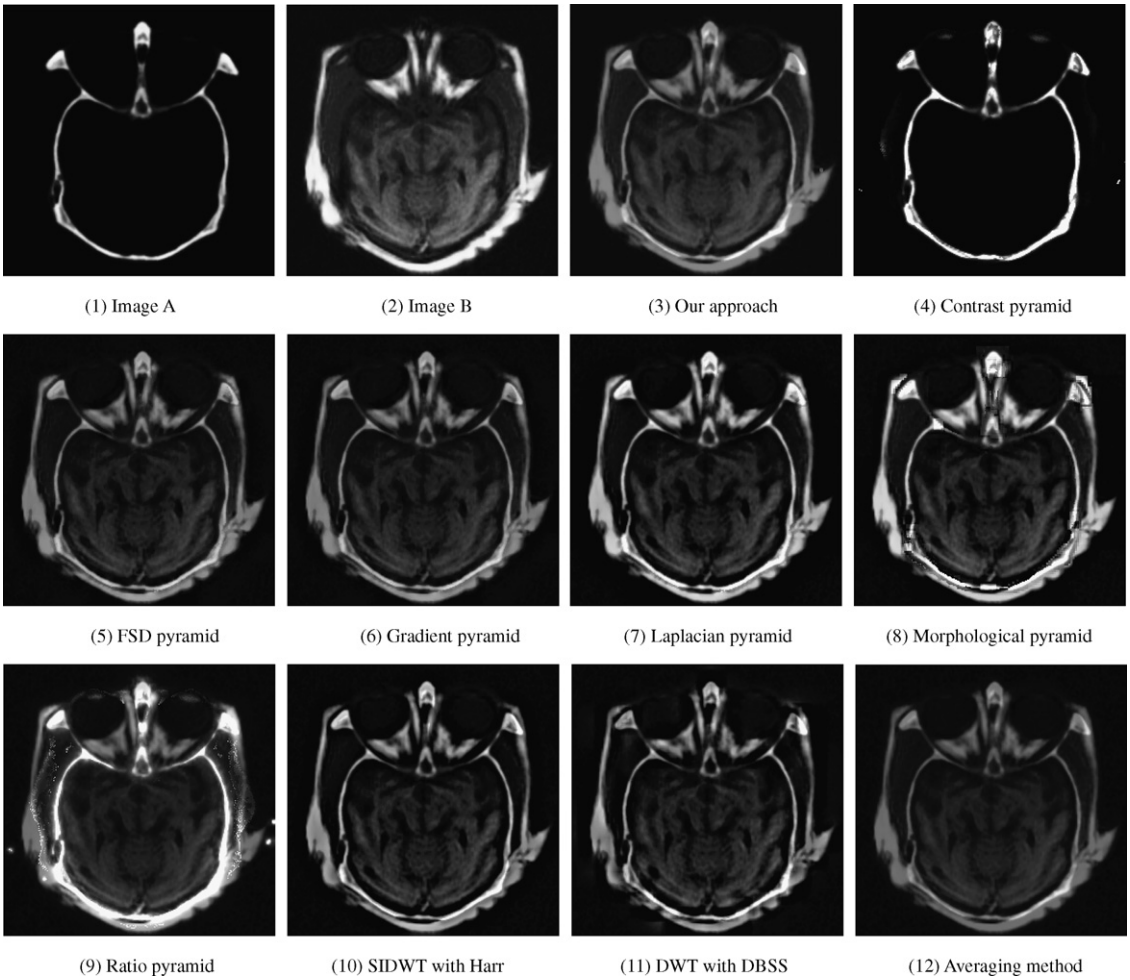

Fig. 3. Group 1 experimental images: (1) and (2) are original images, (3)–(12) are fused images.

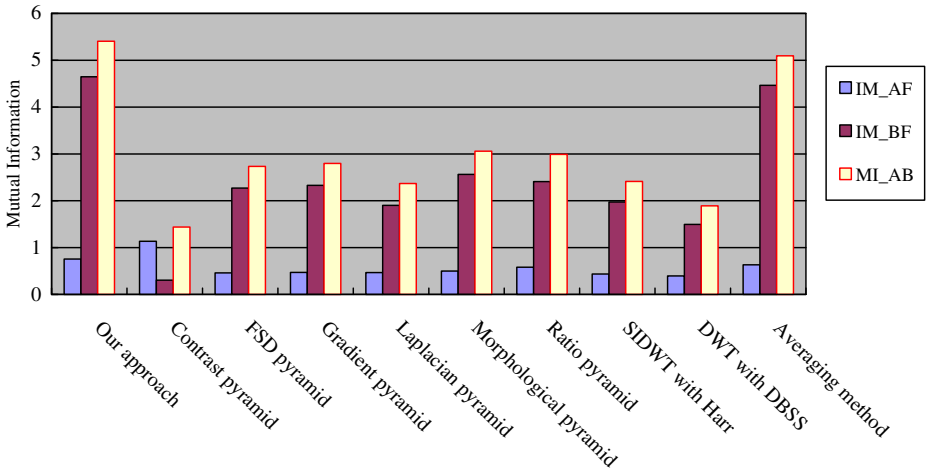

Fig. 4. Group 1: performance of different methods.

not only linear operations but also nonlinear operations in the process of data fusion.

(4) The pulse generator determines the firing events according to the current threshold. Parameter C_n is used to record the number of the firing neuron in the current iteration. Note: each neuron only fires one time in the whole process.

(5) Make $Sum = Sum' + C_n$, where Sum denotes the total number of the fired neurons after the current iteration. Sum' denotes the total number of the fired neurons before the current iteration.

(6) If $Sum < Num$, turn to (2); otherwise, continue. Num means the total number of all neurons in the network.

(7) Normalize the internal state U. The normalized U is the fused image.

Note: because data fusion happens in the internal activity, undoubtedly the internal state U includes all of the fused information needed. But U could not be directly taken as the final output image because some values of U may be out of the dynamic range of the image, making it necessary to adjust U by linear transformation.

4. Results and discussion

In this section, we use m-PCNN to fuse multimodal medical images. Because the parameter setting has an important influence on the performance of the m-PCNN, first, model parameters are given in the experiments. Then, our approach is tested using different medical images and contrasted with other methods of image fusion. Finally, the quality of the fused image is assessed by the universal objective standard.

4.1. Parameter setting

In the experiments, the dual-channel PCNN is taken to fuse different medical images. Its parameters are set as follows: $\beta^1 = \beta^2 = 0.5$; convolution core $K = [0.1091, 0.1409, 0.1091; 0.1409, 0, 0.1409; 0.1091, 0.1409, 0.1091]$; $M(\cdot) = W(\cdot) = Y[n-1] \otimes K$, where $\otimes$ denotes convolution operation; level factor $\sigma = 1.0$; time constant $\alpha_T = 0.012$; and normalized offset parameter $V_T = 4000$.

In order to show the advantages of our method, it is compared with other methods: contrast pyramid, FSD pyramid, gradient pyramid, Laplacian pyramid, morphological pyramid, ratio pyramid, SIDWT with Harr, and DWT with DBSS (2,2). In the experimental images for each group (see 3, 5, 7, and 9), image 1 and image 2 are source images. Image 3 is the fused image using our approach. The six images, in 4–9, are fused by various pyramid algorithms. The last two images are mixed by wavelet transform. Image 10 is obtained by the approach of shift invariant discrete wave transform (SIDWT) with Harr. Image 11 is fused by discrete wavelet transform (DWT), and wavelet is DBSS (2,2). Parameters of these methods are set by: pyramid level = 4, selection rules: high-pass = select max, lowpass = average. Finally, image 12 is obtained by calculating the average of source images.

4.2. Objective standard

For the sake of objectively assessing various methods, we use mutual information as the objective standard to

Table 2
Mutual information of fused images (Group 1)

Methods	MI_AF	MI_BF	MI_AB
Our approach	*0.7556*	*4.6480*	*5.4036*
Contrast pyramid	1.1332	0.3029	1.4361
FSD pyramid	0.4603	2.2721	2.7324
Gradient pyramid	0.4696	2.3282	2.7978
Laplacian pyramid	0.4659	1.9022	2.3681
Morphological pyramid	0.4985	2.5612	3.0597
Ratio pyramid	0.5799	2.4098	2.9897
SIDWT with Haar	0.4369	1.9739	2.4109
DWT with DBSS (2,2)	0.3952	1.4956	1.8907
Averaging method	0.6311	4.4628	5.0939

estimate the performance of different methods. In fact, image fusion is to fuse a variety of multi-source images and aims at creating a fused image that acquires as much information from each of the source images as possible.

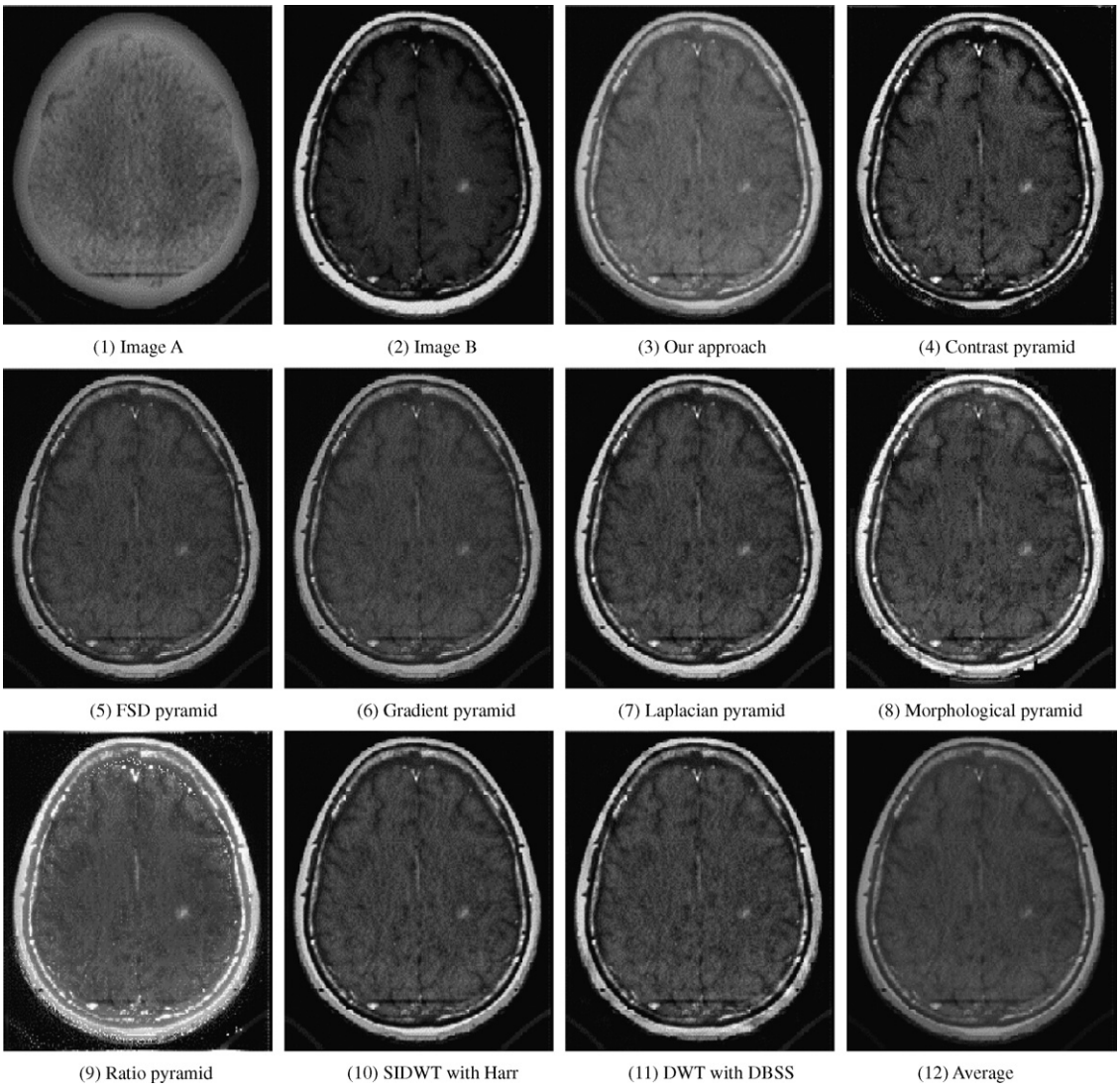

Fig. 5. Group 2 experimental images: (1) and (2) are original images, (3)–(12) are fused images.

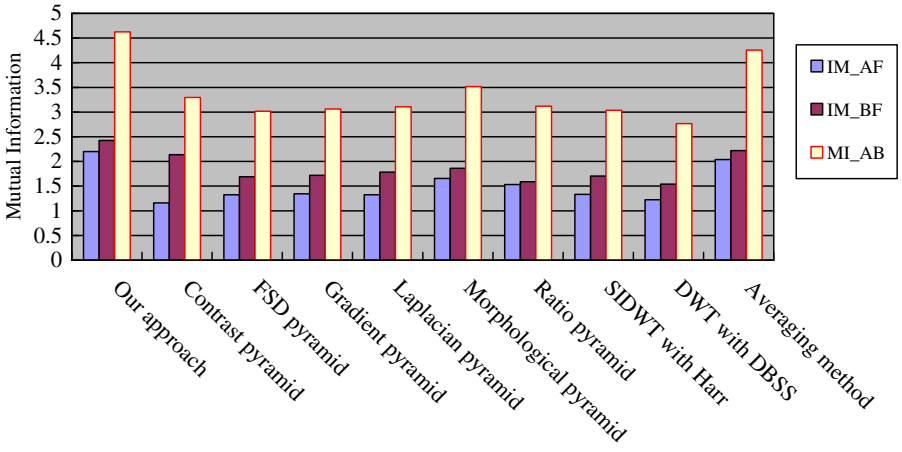

Fig. 6. Group 2: performance of different methods.

The more information obtained from source images, the better the effect of fusion there is. Then, mutual information can measure the similarity between two images. If both sides are similar, the value of mutual information is larger. Hence, mutual information can exactly measure the performance of different methods.

Some terms in the figure and the table are explained. MI_AF denotes mutual information between image A and the fused image; MI_BF denotes mutual information between image B and the fused image; MI_AB denotes the cumulative mutual information and its value is the sum of MI_AF and MI_BF. MI_AB shows the ability to acquire information from image A and image B, so MI_AB is used to evaluate different image fusion methods. A larger MI_AB indicates the fused image acquires more information from image A and image B, than a smaller MI_AB. In other words, the method with a larger MI_AB is superior to others among the various methods.

Table 3
Mutual information of fused images (Group 2)

Methods	MI_AF	MI_BF	MI_AB
Our approach	*2.2014*	*2.4250*	*4.6264*
Contrast pyramid	1.1584	2.1388	3.2972
FSD pyramid	1.3252	1.6907	3.0160
Gradient pyramid	1.3439	1.7187	3.0626
Laplacian pyramid	1.3245	1.7835	3.1080
Morphological pyramid	1.6557	1.8604	3.5161
Ratio pyramid	1.5313	1.5888	3.1201
SIDWT with Haar	1.3338	1.7024	3.0362
DWT with DBSS (2,2)	1.2252	1.5409	2.7661
Averaging method	2.0369	2.2195	4.2564

4.3. Analyses and discussion

To illustrate the proposed fusion method, several experimental results are presented. Experiments are performed on four groups of 256-level images. Each group has a pair of medical images from different sources. The information of each source image is listed in Table 1. For example, images in group 1 are acquired from the same position in the brain using different devices. Image A shown in Fig. 3(1) is a CT image that shows structures of bone, while image B shown in Fig. 3(2) is an MR image that shows areas of soft tissue. However, in clinical applications, doc-

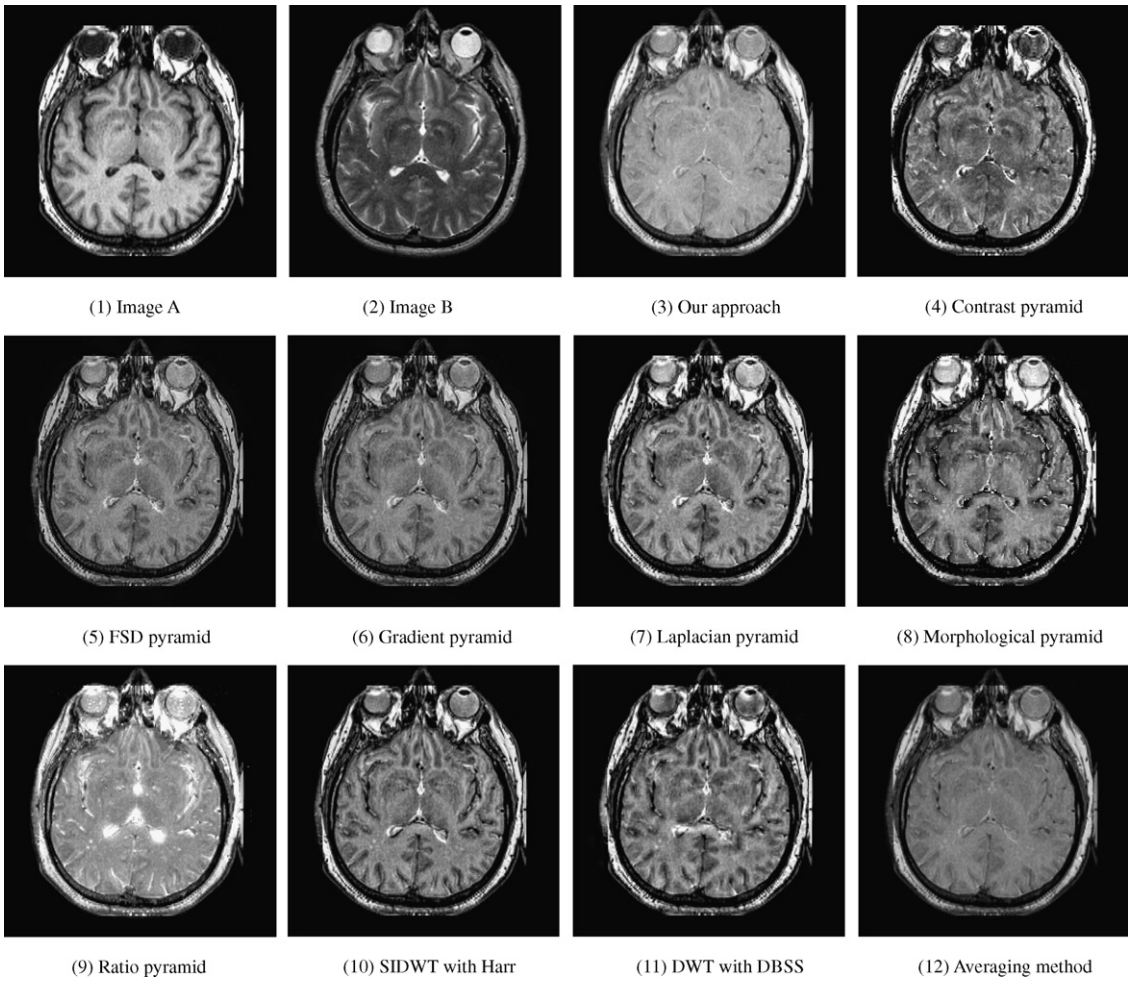

Fig. 7. Group 3 experimental images: (1) and (2) are original images, (3)–(12) are fused images.

tors need to see the position of both bone and tissue to determine pathology and aid in diagnosis. So the mixed image is usually needed in practice, which includes as much of the information in A and B as possible.

From Fig. 3, it is clear that: Fig. 3(4) does not contain the information in image B; Fig. 3(9) contains false information that appears as bright spots, which do not exist in image A or image B; and Fig. 3(7) and (8) have a good contrast, however, looking at Fig. 3(8) carefully, there are also some sharp edges in this figure. Except for these four images, the remaining images seem very similar. The results of objective assessment are shown in Fig. 4 and Table 2. Obviously, our proposed method is superior to others because our MI_AB is the largest, MI_AB = 5.4036. It shows the fused image by our method acquires the most information from image A and image B. Averaging method comes in second place, morphological pyramid method is in the third place, and the effect of contrast pyramid

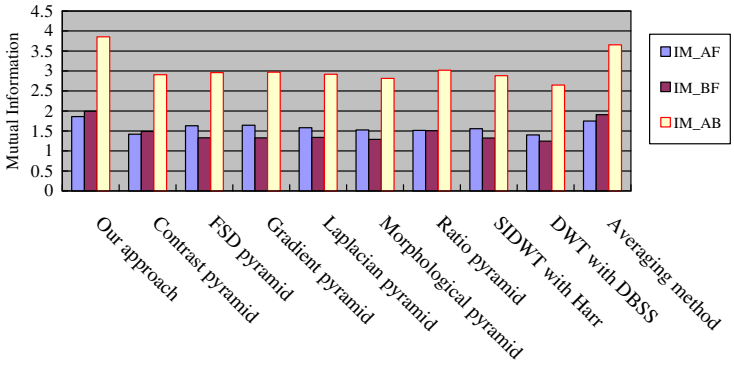

Fig. 8. Group 3: performance of different methods.

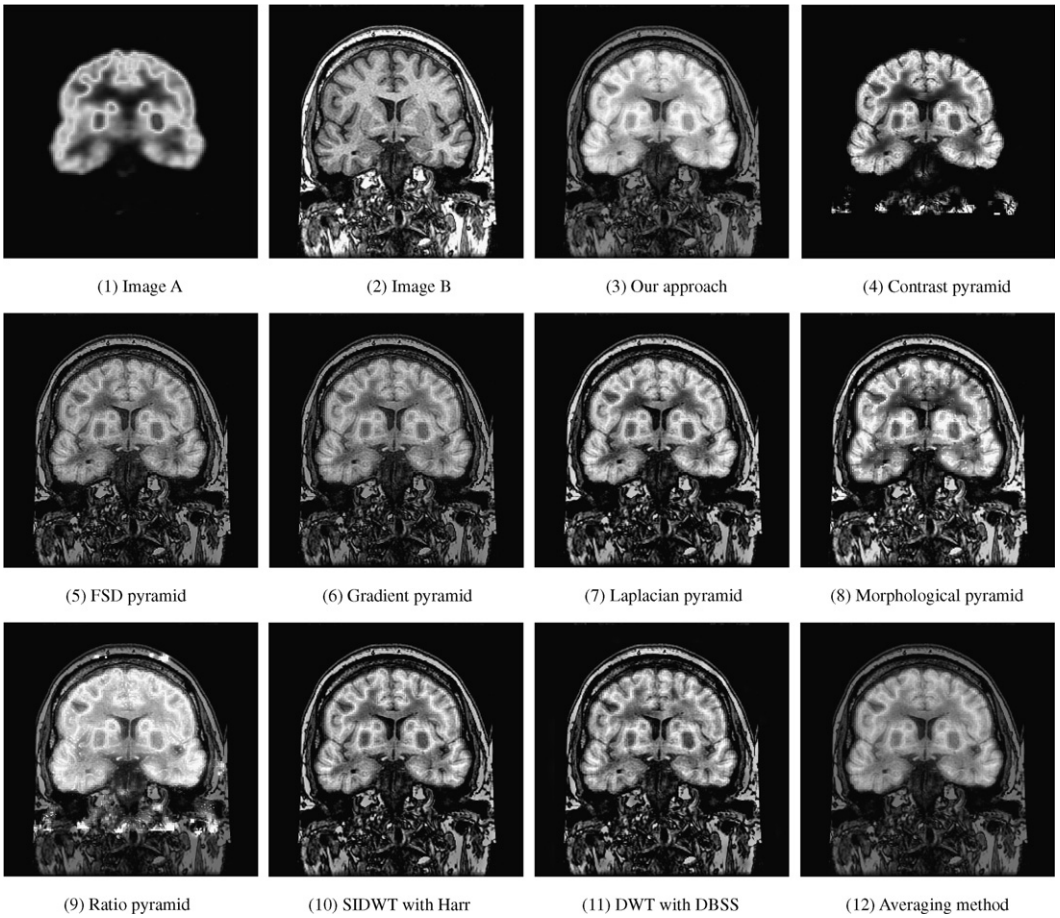

Fig. 9. Group 4 experimental images: (1) and (2) are original images, (3)–(12) are fused images.

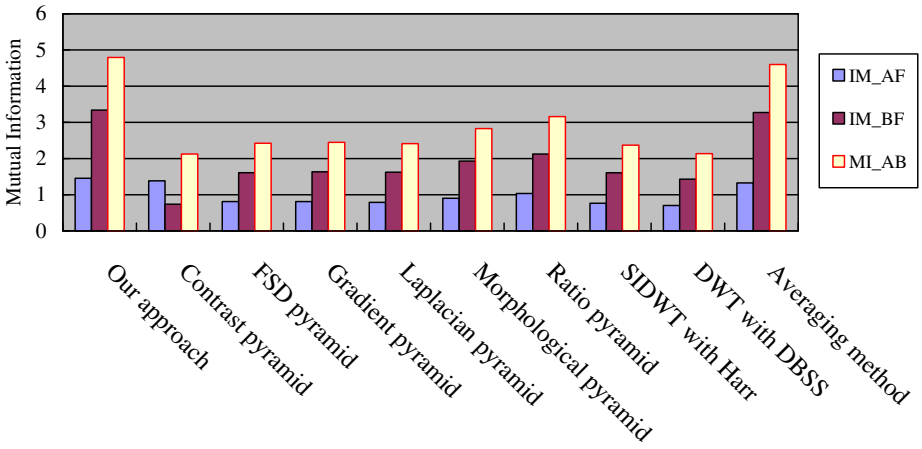

Fig. 10. Group 4: performance of different methods.

method is the worst. Therefore, in group 1 our method is outstanding.

With regard to group 2 shown in Fig. 5, Fig. 5(1) is a CT image and Fig. 5(2) is an MR image. Fused images are shown in Fig. 5(3)–(11). Ratio pyramid method is worse than the others because there are so many bright spots in Fig. 5(9). Fig. 5(4) and (8) have bad edges. Seen from Fig. 6 and Table 3, the fused image obtained by our method has the largest IM_AB, MI_AB = 4.6264. Averaging method and morphological pyramid method lie respectively in the second place and the third place. DWT with DBSS (2, 2) has the smallest mutual information.

In group 3 shown in Fig. 7 and group 4 shown in Fig. 9, Figs. 7(1) and (2) and 9(1) and (2) come from the website of the Atlas project, which is made possible in part by the Departments of Radiology and Neurology at Brigham and Women's Hospital, Harvard Medical School, the Countway Library of Medicine, and the American Academy of Neurology [19]. Fig. 7(1) and (2) are transaxial brain images. The modality of Fig. 7(1) is MR-T1 and the modality of Fig. 7(2) is MR-T2. Fig. 9(1) is a coronal FDG image and Fig. 9(2) is a coronal MR-T1 image.

All the results in group 3 and group 4 are very good except Figs. 7(8), 9(4), and (8). Both Figs. 7(8) and 9(8) have bad edges, and we mostly cannot see Fig. 9(2) in (4), which is the worst result. Nevertheless, the images fused by our method in Figs. 8 and 10 obtain the best results, for they contain the richest information from source images. Here are specific results: IM_AB = 3.8551 in Table 4, IM_AB = 4.7957 in Table 5. Ratio pyramid method comes in third place, while contrast pyramid method lies in the third place in Figs. 4 and 6. Hence, we can see the order of other methods except our approach and averaging method changes in processing different images. It shows those methods have bad flexibility and stability. However, our method is always in first place and the averaging method lies behind it no matter what images are processed. It shows that both our approach and the averaging method are flexible and stable, though

Table 4
Mutual information of fused images (Group 3)

Methods	MI_AF	MI_BF	MI_AB
Our approach	*1.8620*	*1.9931*	*3.8551*
Contrast pyramid	1.4196	1.4881	2.9077
FSD pyramid	1.6310	1.3292	2.9602
Gradient pyramid	1.6443	1.3259	2.9702
Laplacian pyramid	1.5808	1.3373	2.9181
Morphological pyramid	1.5256	1.2907	2.8163
Ratio pyramid	1.5141	1.5065	3.0207
SIDWT with Haar	1.5573	1.3241	2.8814
DWT with DBSS (2,2)	1.4012	1.2471	2.6483
Averaging method	1.7483	1.9063	3.6546

Table 5
Mutual information of fused images (Group 4)

Methods	MI_AF	MI_BF	MI_AB
Our approach	*1.4559*	*3.3398*	*4.7957*
Contrast pyramid	1.3865	0.7379	2.1245
FSD pyramid	0.8130	1.6102	2.4231
Gradient pyramid	0.8141	1.6330	2.4472
Laplacian pyramid	0.7887	1.6224	2.4111
Morphological pyramid	0.9011	1.9292	2.8303
Ratio pyramid	1.0342	2.1254	3.1596
SIDWT with Haar	0.7647	1.6062	2.3709
Averaging method	1.3265	3.2741	4.6006

the averaging method's results cannot acquire more information than our approach.

From the above analysis and discussion, we can draw the conclusion that our method outperforms all the others in the field of medical image fusion. In addition, our method has many advantages. For example, it has good flexibility and high stability. And because it acquires more information from source images, our method is more useful for doctors than the others mentioned above.

On the other hand, we have to acknowledge that our fused image in image definition and contrast is not as good as the image obtained by the Laplacian pyramid method. Although improving the quality of the image is the goal

of image enhancement technology, we do hope to further improve our method to obtain a fused image with even better quality in future work.

5. Conclusion

Medical image fusion plays an important role in clinical applications. But all methods previously proposed do not meet clinical demands completely. In this instance, we propose the *m*-PCNN for the purpose of medical data fusion. As it is a special case, dual-channel model is also introduced. Finally, 4 pairs of medical images are used to test the performance of the *m*-PCNN against other methods and to prove by experimental results that our method is superior to any others.

In the experiments, in order to estimate various methods we take mutual information as the objective estimate standard. The experimental results show our proposed method outperforms the other methods compared and is efficient and very suitable for medical image fusion.

Acknowledgements

The authors thank the associate editor and the anonymous reviewers for their careful work and valuable suggestions for an earlier version of this paper. We also are very grateful to Ying Zhu, who is a postgraduate in the School of Life Sciences, Lanzhou University, who provided many useful suggestions for this paper. At the same time, we are grateful to Allan Grey, the Ph.D. students' foreign English teacher in Lanzhou University, who kindly helped us to correct grammar and spelling mistakes in the paper. Moreover, our work is supported by the National Natural Science Fund (No. 60572011).

References

[1] H. Anderson, A filter-subtract-decimate hierarchical pyramid signal analyzing and synthesizing technique. US Patent 718 104, 1987.
[2] P.J. Burt, A gradient pyramid basis for pattern-selective image fusion, in: Proceedings SID International Symposium, Society for Information Display, Playa del Rey, CA, 1992, pp. 467–470.
[3] P.J. Burt, E.H. Adelson, The Laplacian pyramid as a compact image code, IEEE Transactions on Communications COM-31 (4) (1983) 532–540.
[4] H. Li, B.S. Manjunath, S.K. Mitra, Multisensor image fusion using the wavelet transform, Computer Vision, Graphics and Image Processing: Graphical Models and Image Processing 57 (3) (1995) 235–245.
[5] O. Rockinger, Image sequence fusion using a shift-invariant wavelet transform, in: Proceedings of the IEEE International Conference on Image Processing, 1997, pp. 288–291.
[6] A. Toet, A morphological pyramidal image decomposition, Pattern Recognition Letters 9 (4) (1989) 255–261.
[7] A. Toet, Image fusion by a ratio of low-pass pyramid, Pattern Recognition Letters 9 (4) (1989) 245–253.
[8] A. Toet, J.J. van Ruyven, J.M. Valeton, Merging thermal and visual images by a contrast pyramid, Optical Engineering 28 (7) (1989) 789–792.
[9] R. Eckhorn, H.J. Reitboeck, M. Arndt, P.W. Dicke, A neural network for feature linking via synchronous activity: Results from cat visual cortex and from simulations, in: R.M.J. Cotterill (Ed.), Models of Brain Function, Cambridge Univ. Press, Cambridge, UK, 1989, pp. 255–272.
[10] R. Eckhorn, H.J. Reitboeck, M. Arndt, P.W. Dicke, Feature linking via synchronization among distributed assemblies: Simulation of results from cat cortex, Neural Computation 2 (1990) 293–307.
[11] H.S. Ranganath, G. Kuntimad, J.L. Johnson, Pulse coupled neural networks for image processing, in: Proc. 1995 IEEE Southeast Con, Raleigh, NC, 1995, pp. 37–43.
[12] J.L. Johnson, H.S. Ranganath, G. Kuntimad, H.J. Caulfield, Pulse-coupled neural networks, in: O. Omidvar, J. Dayhoff (Eds.), Neural Networks and Pattern Recognition, Academic, San Diego, CA, 1998, pp. 1–56.
[13] J.L. Johnson, D. Ritter, Observation of periodic waves in a pulse-coupled neural network, Optics Letters 18 (1993) 1253.
[14] J.L. Johnson, M.L. Padgett, PCNN models and applications, IEEE Transactions on Neural Networks 10 (3) (1999).
[15] T. Lindblad, J.M. Kinser, Image Processing Using Pulse-Coupled Neural Networks, second revised ed., Springer, 2005.
[16] Yide Ma, Lian Li, et al., Principle of Pulse-Coupled Neural Network and Its Applications, Science Press, Beijing, China, 2006.
[17] R.P. Broussard, S.K. Rogers, M.E. Oxley, et al., Physiologically motivated image fusion for object detection using a pulse coupled neural network, IEEE Transactions on Neural Networks 10 (3) (1999) 554–563.
[18] Wei Li, Xue-Feng Zhu, A New Image Fusion Algorithm Based on Wavelet Packet Analysis and PCNN, in: Proceedings of the Fourth International Conference on Machine Learning and Cybernetics, Guangzhou, China, 2005, pp. 5297–5301.
[19] http://www.med.harvard.edu/AANLIB.